

Towards crystalline ion beams - the PALLAS¹ ring trap

T.Schätz, D. Habs, C. Podlech, J. Wei* and U. Schramm

Ludwig-Maximilians-Universität München, Sektion Physik, 85748 Garching, Germany
*Brookhaven National Laboratory, Upton, New York 11979

RECEIVED

NOV 20 1998

OSTI

Abstract. To experimentally elucidate fundamental issues of crystalline ion beams at low velocities we presently set up PALLAS¹, a table top circular RF quadrupole storage ring for acceleration and laser cooling of, e.g., $^{24}\text{Mg}^+$ ions. Employing the smooth approximation to PALLAS we compare its beam dynamics to heavy ion synchrotrons like TSR Heidelberg and thereby demonstrate the necessity of the highly symmetric lattice for the attainment of crystalline structures. Furthermore, dedicated molecular dynamics simulations are presented, affirming the feasibility of beam crystallization in PALLAS.

INTRODUCTION

The fascination of crystalline ion beams [1], representing the ultimate form of space charge dominated beams in accelerator physics and reaching far beyond standard limitations of emittance dominated beams, has strongly driven the improvement of storage ring cooling techniques like electron and laser cooling throughout the last decade [2,3]. However, since the first discussion of crystalline ion beams following experiments at the NAP-M proton storage ring [4], no such beam has been definitely proven up to now. Only evidence for the formation of a chain like structure of highly charged ions electron cooled at the ESR [5] as well as a preliminary hint for beam ordering of a longitudinally and dispersively [6] laser cooled $^9\text{Be}^+$ ion beam at the TSR [7] have been reported. On the other hand, early theoretical predictions concerning the structure of ion crystals under storage ring like focusing conditions [8] were confirmed by elaborate studies of ion crystals at rest in traps (see e.g. [9,10]). Regarding especially higher order structures like helices, which are nicely observable in trap experiments, this fact is believed to be due to the too low symmetry and periodicity of the lattice functions of existing storage rings [2,3]. Nevertheless, overcoming shear forces in the bending sections by a well adapted gradient laser cooling and applying direct transverse cooling, low order crystalline structures were proposed to be reachable in the present machines [11]. Here dedicated molecular dynamics (MD) simulations were performed, which, besides full inter-particle Coulomb interaction take into account the individual lattice parameters of any given storage ring.

SMOOTH APPROXIMATION

As depicted in fig. 1, beam heating (or to be more precise emittance growth in the transverse and broadening of the momentum distribution in the longitudinal degree of freedom) in present day heavy ion storage rings originates from the unavoidable polygon-like arrangement of the ring focusing and bending magnets. This feature on the one hand effects orbital variations of the focusing strength, expressed by the β -function, which cause beam envelope oscillations and thus via intra beam scattering (IBS) represents the major heating mechanism. On the other hand shear is introduced predominantly in the bending regions, expressed by the dispersion function D , leading to less important heating in the emittance dominated regime. Since clearly bending but

¹⁾ PAuL Laser cooling Acceleration System

*Work performed under the auspices of the U.S. Department of Energy.

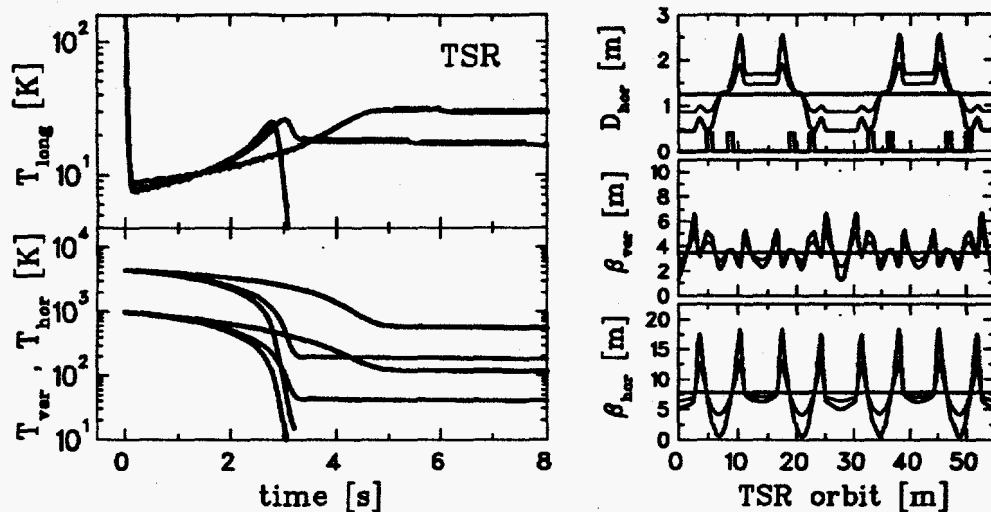


FIGURE 1. Simulation (Code INTRABSC [12]) of the temporal development of the longitudinal (upper figure) and transverse (lower figure) beam temperatures of an uncooled ${}^9\text{Be}^+$ beam ($7 \cdot 10^5$ ions) at the TSR Heidelberg, subjected to longitudinal laser cooling at a typical rate of 0.04 1/s. Regarding realistic conditions (black line) laser cooling leads to a fast reduction of the longitudinal temperature followed by a pronounced indirect transverse cooling [6] mediated by intra beam Coulomb scattering (IBS). The equilibrium temperatures now strongly depend on the heating mechanisms inherent in heavy ion storage rings: The orbital variation (right figures) of the focusing strength (β -function) and therefore of the mean beam radius causes beam heating via IBS as also does (less important) shear (dispersion function D) in the bending regions (the position of the bending dipoles is marked in the upper right figure). Artificially reducing β_{hor} , β_{ver} and D to half amplitude (light grey curves) already illustrates reduced heating. For the smooth approximation (dark grey curves), eliminating local variations of the ring lattice functions, IBS beam heating almost vanishes in the simulation, when the phase space density of the beam is reduced sufficiently.

also focusing primarily acts in the horizontal plane (see right part of fig. 1), longitudinal laser cooling in storage rings generally leads to a strongly anisotropic velocity distribution at rather high equilibrium temperatures [6].

We now apply the smooth approximation to, e.g., the TSR Heidelberg by artificially using the mean values of the corresponding lattice β -functions β_{hor} , β_{ver} and the dispersion function and therefore eliminate the influence of envelope oscillations (dark grey curves in fig. 1). This results in a collapse of the transverse and longitudinal temperatures after a sufficient reduction of the transverse phase space density and thus of the remaining heating rate (due to the const. dispersion). Despite the fact that the temperature region below the latter cannot be reasonably simulated by the employed code INTRABSC [12] (only employing frictional cooling and neglecting static inter-particle Coulomb forces), we want to emphasize the obvious advantage of realizing a *smooth* ring like the RF quadrupole ring PALLAS [13], details described below, for the scope of beam crystallization. A more rigid definition of the validity of the mentioned smooth approximation is given in the following.

The smooth approximation (SA) is a universal approximation method for integrating Hill's equation or generally differential equations with periodic coefficient like

$$\ddot{y} + K(s)y = 0, \quad K(s+L) = K(s). \quad (1)$$

As a general result of this method one, e.g., obtains the wavelength λ of the solution $y(s)$ implying λ to be large compared to the length of the periodic focusing structure L . For an accuracy within a few percent the relation

$$\lambda \gtrsim 2.6 \cdot L \quad (2)$$

has to be satisfied [14]. The position dependent restoring force $-K(s)y$ may then be replaced by an equivalent average restoring force $-\bar{K}y$. To compare this condition with the relevant (compared to an equivalent strong focusing synchrotron) design parameters of the RF quadrupole storage ring PALLAS we introduce [14]: the

DISCLAIMER

This report was prepared as an account of work sponsored by an agency of the United States Government. Neither the United States Government nor any agency thereof, nor any of their employees, makes any warranty, express or implied, or assumes any legal liability or responsibility for the accuracy, completeness, or usefulness of any information, apparatus, product, or process disclosed, or represents that its use would not infringe privately owned rights. Reference herein to any specific commercial product, process, or service by trade name, trademark, manufacturer, or otherwise does not necessarily constitute or imply its endorsement, recommendation, or favoring by the United States Government or any agency thereof. The views and opinions of authors expressed herein do not necessarily state or reflect those of the United States Government or any agency thereof.

DISCLAIMER

Portions of this document may be illegible in electronic image products. Images are produced from the best available original document.

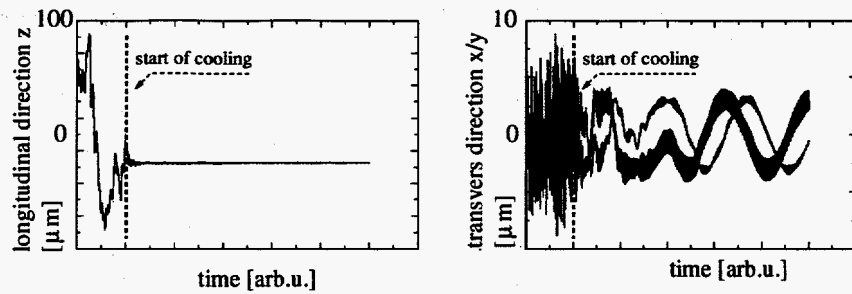


FIGURE 2. Longitudinal respectively transverse position of a test particle in the MD simulation (one out of 10^5 in the whole ring) versus time. While the longitudinal (beam orbit) position coincides with its equilibrium value (co-moving frame) immediately after the beginning of longitudinal cooling, the behavior in both transverse degrees of freedom is different: requiring time for the ordering process, the transverse motion is finally described by two phase shifted oscillations corresponding to a twisting helix-like trajectory.

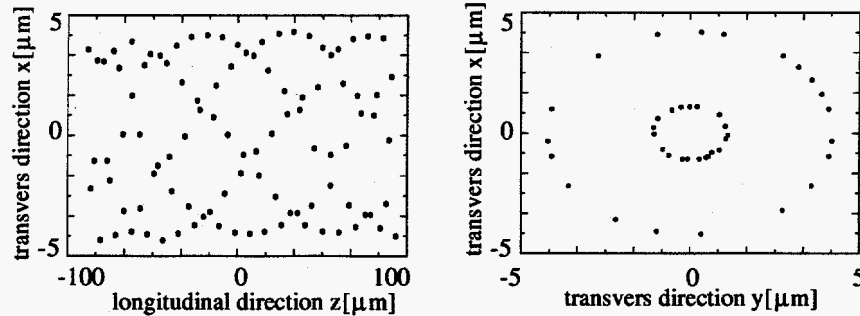


FIGURE 3. Snapshot of the ion distribution in the beam after the phase transition demonstrated in fig. 2 has occurred.

tune Q_x , the average beta function $\beta_{x,y} = \beta_o$, the average dispersion function of the ring D_o , the momentum compaction factor α and the transition energy E_t as

$$\begin{aligned}
 Q_x &= 2\pi R_o \nu_\beta / v_o = 100 \\
 \beta_o &= R_o / Q_x = 5 \cdot 10^{-4} \text{ m} \\
 D_o &= R_o / Q_x^2 = 5 \cdot 10^{-6} \text{ m} \\
 \alpha &= 1 / Q_x^2 = 1 \cdot 10^{-4} \\
 E_t &= Q_x \cdot M c^2 = 2.4 \text{ TeV}
 \end{aligned}
 \tag{3}$$

Here $R_o = 57.5 \text{ mm}$ corresponds to the radius of PALLAS, ν_β to the secular frequency in a RF quadrupole trap, respectively to the betatron frequency in a synchrotron, of 1 MHz (at about 5 MHz driving RFQ frequency), $M c^2$ to the $^{24}\text{Mg}^+$ ion mass and $v_o = 3000 \text{ m/s}$ to the average ion velocity, respectively the kinetic energy of 1 eV. Consequently the centrifugal force will not cause a significant change (of the order of $10 \mu\text{m}$ for a typical secular potential of 10 eV) of the orbital radius of PALLAS. Due to the highly symmetric setup of PALLAS the periodicity length L of the focusing parameter K is less than 1 mm for the given velocity, while the wavelength λ of the betatron oscillation is of the order of 3 mm. Therefore PALLAS fulfills the requirement given in eq. 2 (in contrast to TSR, where $\lambda \gtrsim L$) and will thus be treated according to the SA in dedicated MD simulation of laser cooling of ion beams in PALLAS, presented below.

Fig. 2 qualitatively shows the behavior of one particle out of the sum of 40 in the MD simulation cell, representing 10^5 ions in the storage ring respectively. The longitudinal (beam direction) position of test particle reaches its equilibrium position (in the co-moving frame) rapidly after the beginning of (up to now unrealistically strong) longitudinal cooling (left figure). The transverse motion shows a lengthy transition phase to the ordered regime, where finally the particles trajectory is described by two phase shifted oscillations in the transverse degrees of freedom (right figure), corresponding to a rotating helix-like structure. The turning is believed to be caused by the non-vanishing angular momentum of the initial velocities in the ion cloud. It remains an interesting experimental task, to verify, whether this rotation survives in PALLAS.

In fig. 3 a snapshot of the simulated ion cloud after the phase transition is presented. The left part of the

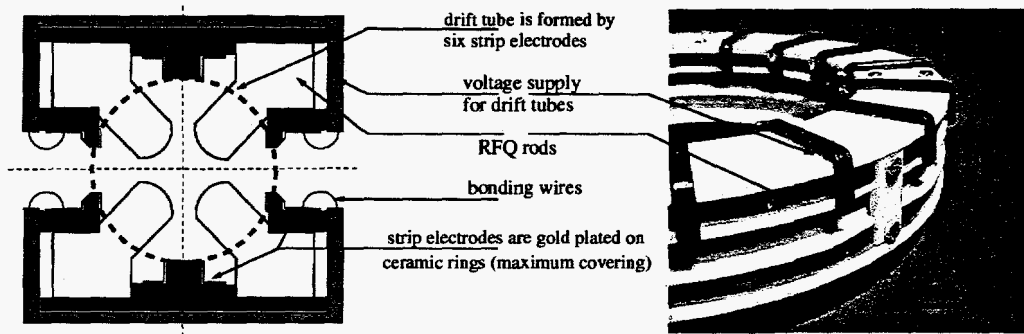


FIGURE 4. Schematic cross section and side view of the present status of the partially assembled PALLAS storage ring: It principally consists out of the four circular RFQ rods providing the storage field on axis and the drift tube arrangement for ion acceleration. The latter are segmented into six stripe electrodes metalized in sandwich layers onto precision Al_2O_3 rings which also guarantee the alignment of the main rods to better than $2/100$ mm. The yokes provide electric contacting of the segments via bonding wires.

figure shows the longitudinal dimension (for simplicity only those ions belonging to the outer helix are shown). The right part shows the transverse cross section of the resulting crystalline beam structure (both helices).

Even though not every possible ion position of the helices comes out to be occupied, the crystalline beam structure remains stable in time. The inter particle distance of about $10 \mu\text{m}$ is comparable to the one observed for corresponding static ion crystals. Varying the ion density, the MD simulation results reasonably follow the crystalline structures, predicted earlier [1].

To now extract the dynamics of beam crystallization and melting (respectively heating and required cooling rates) from ongoing simulations, we have to introduce realistic laser cooling rates and possible external sources for beam heating like patch potentials caused by Mg atoms on the rods, cross talk of disturbing potentials from outside PALLAS and dark ions (e.g. $\text{Mg}^{25/26}$ respectively N^{28}) in the beam.

Summarizing the upper results, we demonstrated the possibility of reaching crystalline beams in PALLAS, employing an approved MD code [11], which was initially developed for the discussion of the stability of crystalline beams in synchrotrons. Obviously one major reason for the predicted stability of higher order crystalline structures is the assumed *smoothness* of the PALLAS lattice, as can be concluded also from the above IBS simulations, where the realistic TSR lattice was compared to an artificially smoothed lattice.

EXPERIMENTAL SETUP

The idea for the PALLAS storage ring has developed starting from the successfully operating RF quadrupole ring trap at the MPQ Munich, where the first beam-like ion crystals of laser cooled $^{24}\text{Mg}^+$ ions were reported [10]. PALLAS now stands for a circular RF quadrupole setup, dedicated especially to the acceleration of stored ions while preserving the established environmental conditions of the ring trap. To visualize the underlying idea, let us assume to start with a 3D crystalline structure at rest. Now forming a crystalline beam were equivalent to rotating the ring trap without affecting the ion crystal due to the high symmetry of the ring, centrifugal forces being negligible in PALLAS, as described in the preceding section. Despite the simplicity of this argument, the realization of crystalline beams in existing RFQ ring traps [10] emerged to be technically impossible, since the light pressure of the cooling lasers was by far not sufficient to overcome potential wells along the beam axis due to, e.g., mechanical or chemical imperfections.

We therefore invented an external acceleration mechanism, based on 16 individually biasable drift tubes evenly distributed along the ring circumference. For practical reasons, each tube consists out of six stripe electrode elements which are metalized onto Al_2O_3 rings, as sketched in the cross section of fig. 4. The efficiency of the proposed acceleration scheme was tested in MD simulations, reported in [13], as also more details of the construction of PALLAS. In addition to this description we want to emphasize further improvements concerning the planned operation of the ion source. To avoid any known heating source, we prepare to use a Mg oven with isotopically enriched ^{24}Mg (from naturally 79 % to 99.9 %) thus reducing the quota of dark ions in the crystal. Furthermore we introduce focusing elements to the electron gun, used for ionizing Mg atoms inside

the ring, to optimize the electron beam quality and prepare a pulsed gun mode, triggered by the zero-crossing of the ion storage field, to avoid a deviation of the electron beam.

With the stored ions then being accelerated, their velocity distribution will be reduced by standard longitudinal laser cooling, employing the closed optical transition between the $3^2S_{1/2} - 3^2P_{3/2}$ levels of 279.6 nm. The detection of the aimed beam crystallization should be possible via the well-known [9] hysteresis behavior of the monitored fluorescence signal within the cycle of beam crystallization and melting.

CONCLUSION

The introduction of the smooth approximation for the description of PALLAS in terms of the synchrotron terminology obviously enables the transfer of theoretical models and methods between the well established ion trap to storage ring communities. With the experimental realization of PALLAS fully satisfying the conditions for the smooth approximation, we predict the existence of stable 3D crystalline ion beam configurations for PALLAS employing a dedicated MD simulation code.

Once obtaining a crystalline ion beam of laser cooled $^{24}\text{Mg}^+$ ions in PALLAS, we may continuously introduce disturbances with the acceleration electrodes to investigate the limit of smooth lattice deviations. Comparing and scaling these planned results from PALLAS (approx. 0.4m circumference) with our simulations based on the smooth approximation should enable the detailed study of the properties of beam crystallization in typical ion storage rings (approx. 50m circumference).

REFERENCES

1. D. Habs and R. Grimm, *Ann. Rev. Nucl. Part. Sci.* 45 (1995) 391.
2. Proc. 31st INFN Eloisatron Workshop, Erice, Italy, 1995, eds. D.M. Maletic and A.G. Ruggiero, World Scientific (1996).
3. Proc. Euroconf. on "Atomic Physics with Highly Charged Ions" I, *Hyp. Int.* 99 (1996) and II, *Hyp. Int.* 108 (1997) and III, *Hyp. Int.* in press (1998).
4. V.V. Parkhomchuk et al., Proc. "Ecool" Karlsruhe 1984, ed. H. Poth, KfK Report No. 3846 (1984) 71 and in [2].
5. M. Steck et al., *Phys. Rev. Lett.* 77 (1996) 3803.
6. I. Lauer et al., *Phys. Rev. Lett.* 81 (1998) 2052 and references therein.
7. M. Weidemüller et al., Max-Planck-Institut für Kernphysik (MPI-K), Heidelberg, contribution to this conference.
8. A. Rahman and J.P. Schiffer, *Phys. Rev. Lett.* 57 (1986) 1133 and R.W. Hasse and J.P. Schiffer, *Annals of Phys.* 203 (1990) 419.
9. H. Walther, *Adv. At. Mol. Opt. Phys.* 31 (1993) 137 and 32 (1994) 379.
10. G. Birkel, S. Kassner and H. Walther, *Nature* 357 (1992) 310.
11. J. Wei, X.-P. Li, A. Sessler, *Phys. Rev. Lett.* 73 (1994) 3089 and in Ref. [2] (1996) 229.
12. R. Giannini and D. Möhl, private communication, following M. Martini, CERN Report PS/84-9 AA (1984) and M. Conte and M. Martini, *Part. Accel.* 17 (1985) 1.
13. T. Schätz, U. Schramm, D. Habs, Proc. 3rd Euroconf. on "Atomic Physics with Stored Highly Charged Ions", Ferrara, Italy, Sept. 22.-26. 1997, *Hyp. Int.* in press (1998).
14. H. Bruck, *Circular Particle Accelerators*, La-TR-72-10 Rev., Los Alamos, reprint, MPI-K, Heidelberg, 1986.